

# Corrosion behaviour of duplex stainless steels containing minor ruthenium additions in reducing acid media

J. H. POTGIETER\*

PPC Technical Services, PO Box 40073, Cleveland, 2022, Johannesburg, South Africa

W. O. BARNARD, G. MYBURG

Department of Physics, University of Pretoria, Pretoria, 0001, South Africa

K. VARGA\*, P. BARADLAI\*

Department of Radiochemistry, University of Veszprém, H-8201 Veszprém, Hungary

L. TOMCSANYI

Department of Physical Chemistry, University of Veszprém, H-8201 Veszprém, Hungary

Received 29 August 1995; revised 17 January 1996

---

The dissolution behaviour, as well as the time, potential and concentration dependence of  $\text{HSO}_4^-$ / $\text{SO}_4^{2-}$  and  $\text{Cl}^-$  accumulations measured by an *in situ* radiotracer method on surface oxide-layers of duplex stainless steels containing various amounts of ruthenium as additive are presented and discussed. Several independent techniques, such as mass loss tests, potentiodynamic responses, radiotracer and ICP methods, were used to characterize the complex features of the passivation phenomena of steels modified with ruthenium. The experimental results reveal that the interaction of bisulfate/sulfate ions with passive oxide layer is stronger than those of chloride ions on the stainless steels studied. Both the extent and the strong character of bisulfate/sulfate accumulation are more likely related to the redistribution of the main alloying components (Cr, Ni, Mo) as well as the Ru in the surface oxide-film formed on steels passivated spontaneously in dilute HCl and  $\text{H}_2\text{SO}_4$ . It is found that the ruthenium additions to the base duplex stainless steel significantly increase the corrosion resistance in reducing acid environments. There is evidence of anodic inhibition and this seems to be responsible for the observed increased corrosion resistance of the duplex stainless steels with small ruthenium additions.

---

## 1. Introduction

Alloying of stainless steels with minor amounts of platinum group metals (PGMs) is a very successful way of improving their corrosion resistance in reducing acid media. This technique is known as cathodic modification and its mechanism [1], as well as the various alloy systems to which it has been applied [2], has been described in literature. However, very little work has been reported on the corrosion behaviour of cathodically modified duplex stainless steels [3].

This paper, therefore, reports the results of an investigation into the effect of ruthenium additions on the dissolution behaviour of duplex stainless steels in reducing acid media. A combination of electrochemical, analytical and surface analysis techniques have been used to gain an insight into passivation phenomena and the role of  $\text{Cl}^-$  and  $\text{SO}_4^{2-}$  ions in its breakdown. An important objective of this investigation has been to contribute to a better understanding

of the role of different elements in the whole corrosion process.

## 2. Experimental procedure

### 2.1. Materials

The alloys used in this investigation were melted in a vacuum induction furnace. Chemical analyses of these experimental alloys are shown in Table 1. Since no deliberate nitrogen additions were made, it was necessary to increase the nickel to a higher content than in similar type commercial alloys to obtain an alloy consisting of approximately equal amounts of ferrite and austenite. Each cast ingot was hot-rolled to a plate with a thickness of between 3 mm and 6 mm, then solution annealed for 1 h at 1060 °C and water quenched.

### 2.2. Mass-loss tests

Mass-loss tests to determine the corrosion rate were

\* Authors to whom correspondence should be addressed.

Table 1. Chemical composition of the materials studied in percentages by mass\*

Alloy	Target composition	Cr	Ni	Mo	Ru	Mn	Si	S	P	O	N	C
2209A	Fe-22%Cr-9%Ni-3%Mo-0%Ru	22.0	9.07	2.81	—	0.1	0.070	0.01	0.01	0.021	0.006	0.03
2209B	Fe-22%Cr-9%Ni-3%Mo-0.1%Ru	22.1	9.20	2.89	0.14	0.1	0.025	0.01	0.01	0.042	0.006	0.03
2209C	Fe-22%Cr-9%Ni-3%Mo-0.2%Ru	22.4	9.14	2.82	0.22	0.1	0.030	0.01	0.01	0.050	0.004	0.03
2209D	Fe-22%Cr-9%Ni-3%Mo-0.3%Ru	22.4	9.24	2.92	0.28	0.1	0.030	0.01	0.01	0.037	0.005	0.02

\* The balance of the alloys was Fe.

Table 2. Corrosion rates of duplex stainless steel containing varying amounts of ruthenium in different acid concentrations at 25 °C

Acid	Temp/°C	Concentration /mol dm <sup>-3</sup>	Corrosion rate/μm/year			
			0% Ru	0.14% Ru	0.22% Ru	0.28% Ru
HCl	25	0.55 (1%)	1.70	1.70	0.00	0.00
		1.40 (2%)	327	310	56.8	7.90
H <sub>2</sub> SO <sub>4</sub>	25	0.1 (~ 1%)	0.00	0.00	0.00	0.00
		1.0 (~ 10%)	4.00	4.00	5.20	0.00
		2.0 (~ 20%)	5.80	5.60	3.40	0.00
HCl	55	0.55 (1%)	18.5	10.1	9.90	9.60
		1.40 (2%)	752	710	504	353
H <sub>2</sub> SO <sub>4</sub>	55	0.1 (~ 1%)	3.60	4.30	4.30	0.00
		1.0 (~ 10%)	5.60	6.80	4.30	0.00
		2.0 (~ 20%)	40.9	14.4	12.5	0.00

carried out according to ASTM standards [4]. Suitable sized specimens were cut from each plate, polished to a 120-grit finish and rinsed in distilled water and isopropanol before their masses and dimensions were recorded. All solutions to which the specimens were exposed, were deaerated for at least 30 min before each test was carried out as well as during the test. After completion of each test, the specimens were removed from the solution, mechanically cleaned with a nylon hair brush, rinsed in distilled water and isopropanol before they were dried and reweighed. Corrosion rates calculated from the mass-loss test for each of the different alloys are summarized in Table 2.

### 2.3. Electrochemical measurements

**2.3.1. Potentiodynamic behaviour.** Discs cut from the plate and mounted in suitable electrode holders were polished down to a 1 μm diamond finish. The electrochemical cell consisted of a working electrode, a saturated calomel reference electrode and two graphite counter electrodes. Each sample was initially reduced at -800 mV for 5 min to remove the air-formed oxide. The potential against time was then recorded for each sample until a steady state open-circuit corrosion potential was reached. A potentiodynamic scan was then initiated from -250 mV vs  $E_{\text{corr}}$  and continued in the anodic direction to approximately +1300 mV vs SCE at a scan rate of 0.2 mV s<sup>-1</sup>. All scans were recorded on a PAR 273 potentiostat and characteristic corrosion parameters were calculated with standard software programmes. All solutions were de-aerated and no  $iR$  compensation was employed, since all solutions were highly conducting. Temperature was maintained at 25 ± 1 °C with a waterbath.

**2.3.2. Surface accumulation behaviour.** Accumulation of HSO<sub>4</sub><sup>-</sup>/SO<sub>4</sub><sup>2-</sup> and Cl<sup>-</sup> ions was studied on powdered steel samples by an *in situ* radiotracer method. The main features of the experimental technique, as well as the basic principles of the method, were described previously [5]. Distilled water and analytically pure reagents (from Merck) were used to prepare all solutions. H<sub>2</sub>SO<sub>4</sub> labelled with S-35 (molar activity: 1.8 × 10<sup>9</sup> Bq mmol<sup>-1</sup>) as well as HCl labelled with Cl-36 (molar activity: 2 × 10<sup>7</sup> Bq mmol<sup>-1</sup>) were supplied by Du Pont. Some characterizing data of the system studied by radio active labelling are given in Table 3. Potential values quoted in these studies are given on reference hydrogen electrode scale (RHE).

**2.3.3. Dissolution behaviour of main alloying components.** Concentrations of Fe, Cr, Ni and Mn dissolved from the duplex steel samples were determined in the solutions using an ICP optical emission spectrometer (type of ICP-OES instrument: ARL 3410). For these measurements powdered steel samples were used. The concentration of sulfuric acid ranged from 0 to 1 × 10<sup>-3</sup> mol dm<sup>-3</sup> in 0.1 mol dm<sup>-3</sup> HClO<sub>4</sub> supporting electrolyte.

## 3. Results and discussion

### 3.1. Mass-loss tests

From the mass test results summarized in Table 2 it is clear that the duplex stainless steels corrode much faster in the hydrochloric acid than in the sulfuric acid medium. In both media the addition of increasing amounts of ruthenium had a beneficial

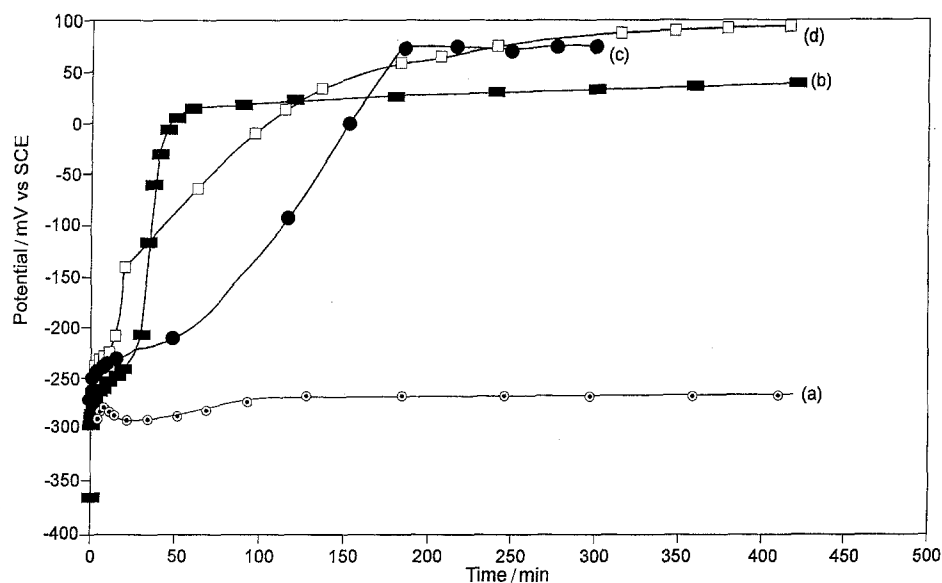
Table 3. Some characterizing data of the system studied by in situ radiotracer technique

Type of species studied	$E\beta_{MAX}/\text{keV}$	Mass-absorption coefficient, $ \text{cm}^2 \text{g}^{-1}$	Characteristic dimensions of the steel samples			Range of concentration $ \text{mol dm}^{-3}$
			Thickness $ \text{mg cm}^{-2}$	Powder diam. $ \mu\text{m}$	Roughness factor	
$\text{H}_2\text{SO}_4$ labelled with $^{35}\text{S}$	167	320*	15	<56	2.24	$5 \times 10^{-6}$ – $1 \times 10^{-3}$
HCl labelled with $^{36}\text{Cl}$	710	34	81	<56	11.19	$2 \times 10^{-5}$ – $2 \times 10^{-2}$

\* Measured value.

Table 4. Important electrochemical parameters of 22% Cr duplex stainless steels derived from their potentiodynamic responses in  $1 \text{ mol dm}^{-3}$   $\text{H}_2\text{SO}_4$  at  $25^\circ\text{C}$ 

Alloy composition	$E_{corr}/\text{mV}$	$i_{corr}/\text{A m}^{-2}$	$i_{pass}/\text{A m}^{-2}$
Fe–22%Cr–9%Ni–3%Mo–0%Ru	–195	$25.8 \times 10^{-2}$	$5.0 \times 10^{-2}$
Fe–22%Cr–9%Ni–3%Mo–0.14%Ru	110	$2.9 \times 10^{-2}$	$1.0 \times 10^{-1}$
Fe–22%Cr–9%Ni–3%Mo–0.22%Ru	158	$1.8 \times 10^{-2}$	$2.0 \times 10^{-1}$
Fe–22%Cr–9%Ni–3%Mo–0.28%Ru	165	$0.7 \times 10^{-3}$	$2.5 \times 10^{-2}$

Fig. 1. Potential–time response curves for a series of duplex stainless steels in  $1 \text{ mol dm}^{-3}$   $\text{H}_2\text{SO}_4$  at  $25^\circ\text{C}$ . Key: (a) 0% Ru, (b) 0.14% Ru, (c) 0.22% Ru and (d) 0.28% Ru.

effect in decreasing the corrosion rate, especially at the highest addition of 0.28% Ru. Provided that a certain minimum concentration of Ru is present, in this case 0.22% Ru at both test temperatures and for HCl concentrations up to 2%, the effect of ruthenium in increasing the corrosion resistance is especially evident in the HCl solutions and at elevated temperature.

### 3.2. Electrochemical behaviour

Figure 1(a)–(d) shows the open-circuit corrosion potential variation of the various duplex stainless steels in  $1 \text{ M H}_2\text{SO}_4$  at room temperature. The potential of the alloys are displaced towards more noble values by the addition of small amounts of ruthenium. All the alloys containing ruthenium passivated spontaneously and stabilized at electro-positive potentials, while the base alloy remained at an electronegative potential value. Figure 2 shows the potentiodynamic curves of these same alloys in

$1 \text{ M H}_2\text{SO}_4$  at  $25^\circ\text{C}$ , while Table 4 summarizes some important electrochemical parameters derived from these responses. Only the base alloy of the duplex stainless steels showed active-to-passive transition behaviour; all the others with Ru additions passivated directly. Decreases in the corrosion current density are observed with an increase in the amount of ruthenium in the alloys and this effect is most prominent in the alloy containing 0.28% Ru. It seems as though the ruthenium additions inhibit the anodic dissolution of the alloys, an observation that is in agreement with previous findings [6].

The response of the duplex stainless steels containing small ruthenium additions is quite different in  $1 \text{ M HCl}$  at  $25^\circ\text{C}$  from their behaviour in sulfuric acid at the same temperature. Figure 3(a)–(d) indicates that none of the alloys passivate spontaneously in  $1 \text{ M HCl}$  solution at room temperature. In fact, all the alloys corroded actively and stabilized at highly electronegative potentials. There is nevertheless still a replacement of the stable open-circuit corrosion

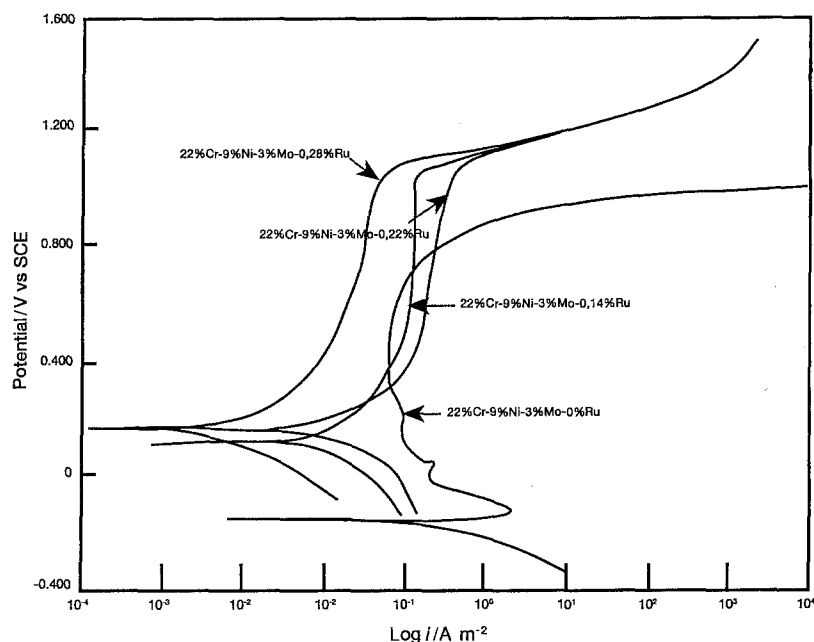


Fig. 2. Potentiodynamic curves for a series of duplex stainless steels in  $1 \text{ mol dm}^{-3} \text{ H}_2\text{SO}_4$  at  $25^\circ\text{C}$ . Key: (a) 0% Ru, (b) 0.14% Ru, (c) 0.22% Ru and (d) 0.28% Ru.

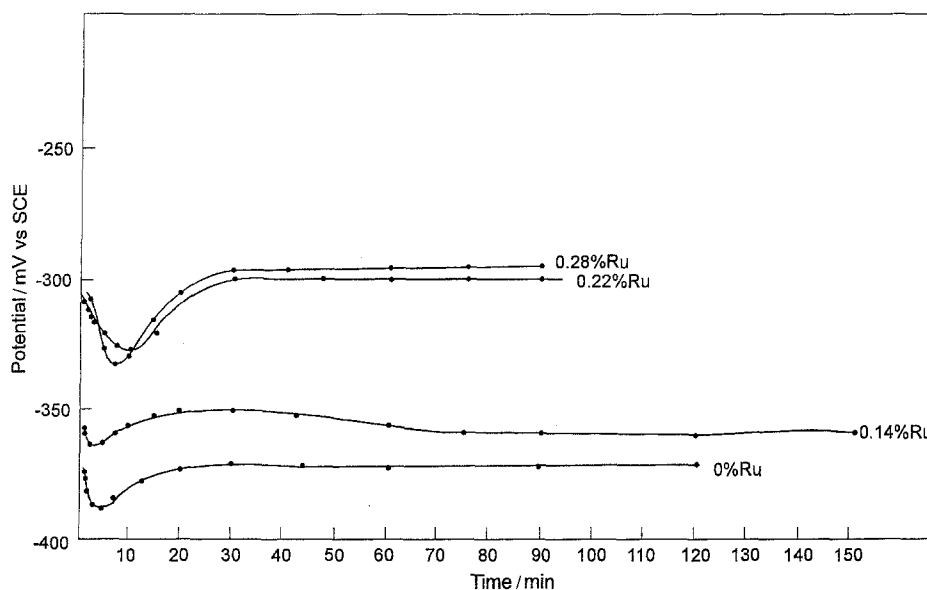


Fig. 3. Potential-time response curves for a series of duplex stainless steels in  $1 \text{ mol dm}^{-3} \text{ HCl}$  at  $25^\circ\text{C}$ . Key: (a) 0% Ru, (b) 0.14% Ru, (c) 0.22% Ru and (d) 0.28% Ru.

potentials towards more noble values with an increase in the ruthenium contents of the alloys.

The anodic potentiodynamic behaviour of these alloys under similar conditions is displayed in Figure 4(a)–(d), while some electrochemical parameters derived from these curves are given in Table 5. In these runs only the anodic responses were recorded because of very severe corrosion of the alloys during exposure to the hydrochloric acid solution. None of the alloys passivated spontaneously, in fact they all corroded actively and all displayed active to passive transition behaviour upon polarization. The critical current density decreases with increasing ruthenium content, demonstrating very clearly that ruthenium inhibits the anodic dissolution process.

### 3.3. Sorption behaviour of duplex steels in $\text{H}_2\text{SO}_4$ and $\text{HCl}$ solutions

The passivation phenomena of duplex stainless steels modified with ruthenium was investigated by measuring the  $\text{HSO}_4^-/\text{SO}_4^{2-}$  and  $\text{Cl}^-$  accumulations with an *in situ* radiotracer method. Powdered stainless steel samples were exposed to dilute reducing acid solutions in which they passivated spontaneously in order to try and gain a better understanding of the role of different elements in the whole corrosion process. Figure 5 shows the time dependence of  $\text{Cl}^-$  sorption measured on two of the duplex stainless steels. The surface concentration of  $\text{Cl}^-$  ions on both steels are small (less than  $\Gamma = 1 \times 10^{-10} \text{ mol cm}^{-2}$ ) and the study of the mobility of labelled chlorides accumulated on duplex

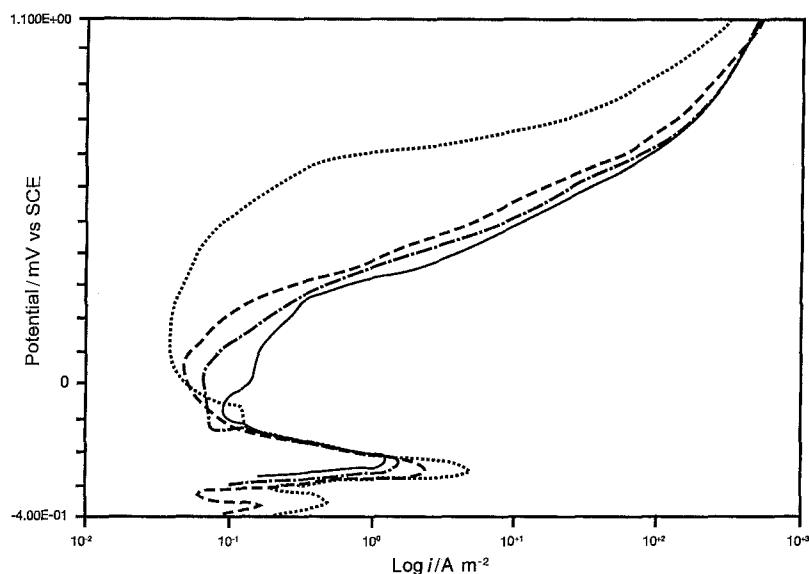


Fig. 4. Potentiodynamic curves for a series of duplex stainless steels in  $1 \text{ mol dm}^{-3}$  HCl at  $25^\circ\text{C}$ . Key: (.....) original 0% Ru; (----) 0.14% Ru; (-.-.-) 0.22% Ru; (—) 0.28% Ru.

Table 5. Important electrochemical parameters of 22% Cr duplex stainless steels derived from their anodic potentiodynamic responses in  $1 \text{ mol dm}^{-3}$  HCl at  $25^\circ\text{C}$

Alloy composition	$E_{\text{corr}}/\text{mV}$	$i_{\text{crit}}/\text{A m}^{-2}$
Fe-22%Cr-9%Ni-3%Mo-0%Ru	-371	5
Fe-22%Cr-9%Ni-3%Mo-0.14%Ru	-360	2.5
Fe-22%Cr-9%Ni-3%Mo-0.22%Ru	-309	1.5
Fe-22%Cr-9%Ni-3%Mo-0.28%Ru	-297	0.12

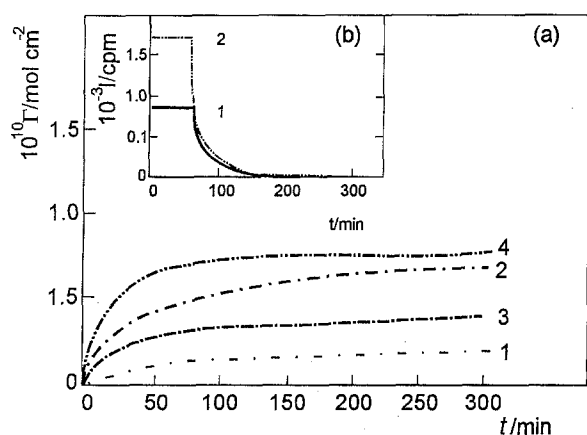


Fig. 5.  $\Gamma$  against time curves of  $\text{Cl}^-$  accumulation in  $0.1 \text{ mol dm}^{-3}$   $\text{HClO}_4$  under open-circuit conditions: (a) (1) and (2) on duplex stainless steel with no Ru at  $\text{Cl}^-$  concentrations of  $2 \times 10^{-5}$  and  $1 \times 10^{-4} \text{ mol dm}^{-3}$ , respectively; (3) and (4) on duplex stainless steel containing 0.28% Ru at  $\text{Cl}^-$  concentrations of  $2 \times 10^{-5}$  and  $1 \times 10^{-4} \text{ mol dm}^{-3}$ , respectively. (b) Study of the mobility of labelled  $\text{Cl}^-$  ions accumulated on duplex steels with 0 and 0.28% Ru (curves (1) and (2), respectively) by addition of the large excess of non-labelled HCl ( $C = 1 \times 10^{-2} \text{ mol dm}^{-3}$ ).

stainless steel (Fig. 5(b)) indicated that no strong embedding of  $\text{Cl}^-$  ions occur. The bisulfate/sulfate accumulation on both duplex stainless steels is graphically depicted in Fig. 6 and indicates a saturation surface concentration of about  $4.5 \times 10^{-10} \text{ mol cm}^{-2}$ . The results of the exchange of labelled  $\text{HSO}_4^-/\text{SO}_4^{2-}$  ions sorbed on duplex stainless steels (curve 3(b) in Fig. 6(a) and curve 1(b) in

Fig. 6(b)) reveal that part of the sulfate-bisulfate species is strongly bonded to the passive layers formed upon spontaneous passivation.

To gain further information on the competitive sorption processes in solutions containing  $\text{Cl}^-$  and  $\text{HSO}_4^-/\text{SO}_4^{2-}$  ions, attempts were made to study the mobility of species accumulated on both duplex stainless steels. Results obtained on the duplex stainless steel with 0.28% Ru are shown in Fig. 7. While at quasiequilibrium conditions it was observed that the surface excesses of bisulfate/sulfate ions on the surfaces of both steels are not influenced by the large excess of  $\text{Cl}^-$  ions (Fig. 7(a)). However, an addition of a small amount of  $\text{HSO}_4^-/\text{SO}_4^{2-}$  ions to the solution

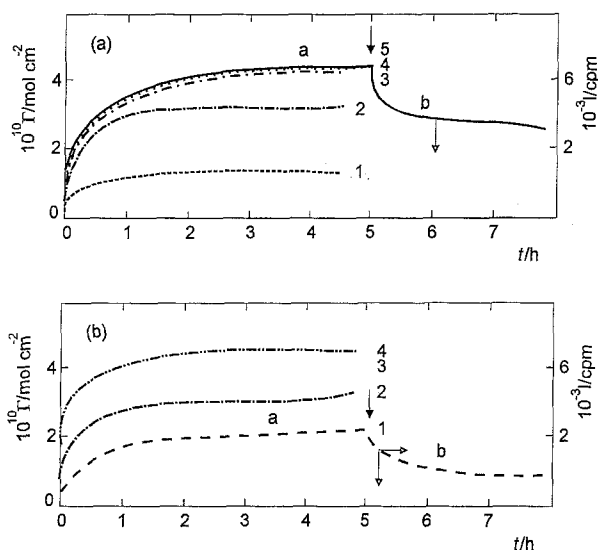


Fig. 6.  $\Gamma$  against time curves of  $\text{H}_2\text{SO}_4$  accumulation in  $0.1 \text{ mol dm}^{-3}$   $\text{HClO}_4$  at open-circuit potentials. (a) On duplex stainless steel with 0% Ru: (1)  $5 \times 10^{-6}$ ; (2)  $1 \times 10^{-5}$ ; (3a)  $2 \times 10^{-5}$ ; (4)  $1 \times 10^{-4}$  (5)  $1 \times 10^{-3} \text{ mol dm}^{-3}$  labelled  $\text{H}_2\text{SO}_4$ ; (3b) addition of  $1 \times 10^{-2} \text{ mol dm}^{-3}$  nonlabelled  $\text{H}_2\text{SO}_4$ . (Open-circuit potentials were shifted in the range of  $-50$  to  $700 \text{ mV}$ .) (b) On duplex stainless steel with 0.28% Ru: (1a)  $5 \times 10^{-6}$ ; (2)  $2 \times 10^{-5}$ ; (3)  $1 \times 10^{-4}$ ; (4)  $5 \times 10^{-4} \text{ mol dm}^{-3}$  labelled  $\text{H}_2\text{SO}_4$ ; (1b) addition of  $1 \times 10^{-2} \text{ mol dm}^{-3}$  nonlabelled  $\text{H}_2\text{SO}_4$ . (Open-circuit potentials were shifted in the range of  $-80$  to  $720 \text{ mV}$ .)

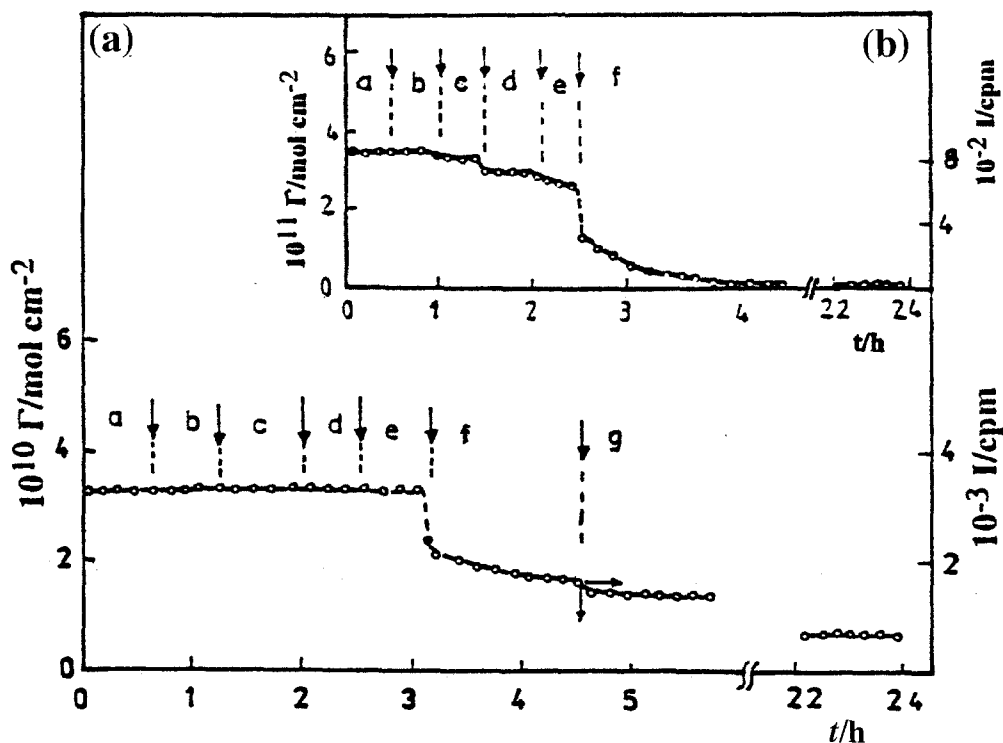


Fig. 7. (a) Effects of HCl additions on the surface concentration of bisulfate/sulfate ions accumulated on duplex stainless steel with 0.28% Ru open-circuit conditions. ( $C = 2 \times 10^{-3} \text{ mol dm}^{-3}$ .) Concentrations of HCl: (a) 0; (b)  $1 \times 10^{-5}$ ; (c)  $2 \times 10^{-5}$ ; (d)  $2 \times 10^{-4}$ ; (e)  $1 \times 10^{-3} \text{ mol dm}^{-3}$ ; (f)–(g) additions of  $1 \times 10^{-2} \text{ mol dm}^{-3}$   $\text{Na}_2\text{CrO}_4$  and nonlabelled  $\text{H}_2\text{SO}_4$ , respectively. (b) Effects of  $\text{H}_2\text{SO}_4$  additions on the surface concentration of chloride ions accumulated on duplex stainless steel with 0.28% Ru at open-circuit conditions. ( $C_{\text{HCl}} = 2 \times 10^{-3} \text{ mol dm}^{-3}$ .) Concentrations of  $\text{H}_2\text{SO}_4$ : (a) 0; (b)  $5 \times 10^{-6}$ ; (c)  $2 \times 10^{-5}$ ; (d)  $2 \times 10^{-4}$ ; (e)  $2 \times 10^{-3} \text{ mol dm}^{-3}$  (f) addition of  $1 \times 10^{-2} \text{ mol dm}^{-3}$  nonlabelled HCl.

phase results in a significant decrease in the values of labelled  $\text{Cl}^-$  accumulated (Fig. 7(b)). These give a strong indication that: (i) only a very limited part of the real surface area of the steel samples is occupied by  $\text{Cl}^-$  ions (pitting corrosion sites); (ii) sorption of  $\text{HSO}_4^-/\text{SO}_4^{2-}$  ions most likely takes place on the total real surface of steel samples (large surface coverage and buildup); (iii) adsorbability of  $\text{HSO}_4^-/\text{SO}_4^{2-}$  ions is significantly higher than that of  $\text{Cl}^-$  ions. From the results it is clear that the Ru content does not exert significant effects on the sorption behaviours of the duplex stainless steel surfaces in either type of acid solution.

Since there is no notable difference between the sorption behaviours of duplex stainless steels (types 0% Ru and 0.28% Ru) studies by *in situ* radio tracer method, it is not surprising that the dissolution rates of the main alloying components at open-circuit corrosion potential are almost the same in the case of both steel samples. The ICP–OES results shown in Figs 8 and 9 reveal the following. (i) The rate of Fe dissolution as well as the amount of Fe dissolved from both duplex steels are two orders of magnitude larger than those found for other alloying elements such as Cr, Ni and Mn. (ii) Solution concentrations of a given alloying component (e.g., Fe or Cr) dissolved from both duplex steels are the same, irrespectively whether the steel sample was alloyed with Ru or not. This may most likely be ascribed to the relatively high content of Mo in the specimens studied. (It is assumed that Mo not only retards anodic dissolution, but also increases the rate of the

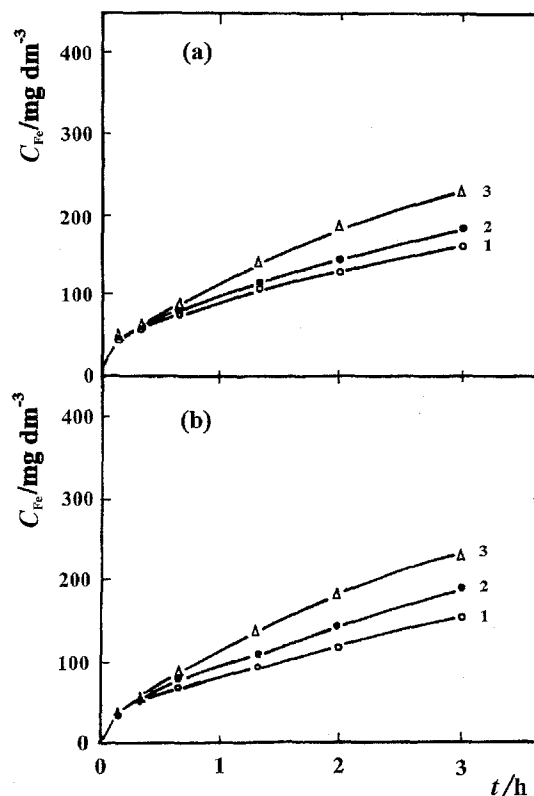


Fig. 8. Time dependence of Fe dissolution measured by ICP optical emission spectrometer upon spontaneous passivation of duplex stainless steel types (a) 0% Ru and (b) 0.28% Ru in solution consisting of (1)  $0.1 \text{ mol dm}^{-3} \text{ HClO}_4$ ; (2)  $0.1 \text{ mol dm}^{-3} \text{ HClO}_4 + 2 \times 10^{-3} \text{ mol dm}^{-3} \text{ H}_2\text{SO}_4$ ; (3)  $0.1 \text{ mol dm}^{-3} \text{ HClO}_4 + 1 \times 10^{-3} \text{ mol dm}^{-3} \text{ H}_2\text{SO}_4$ .

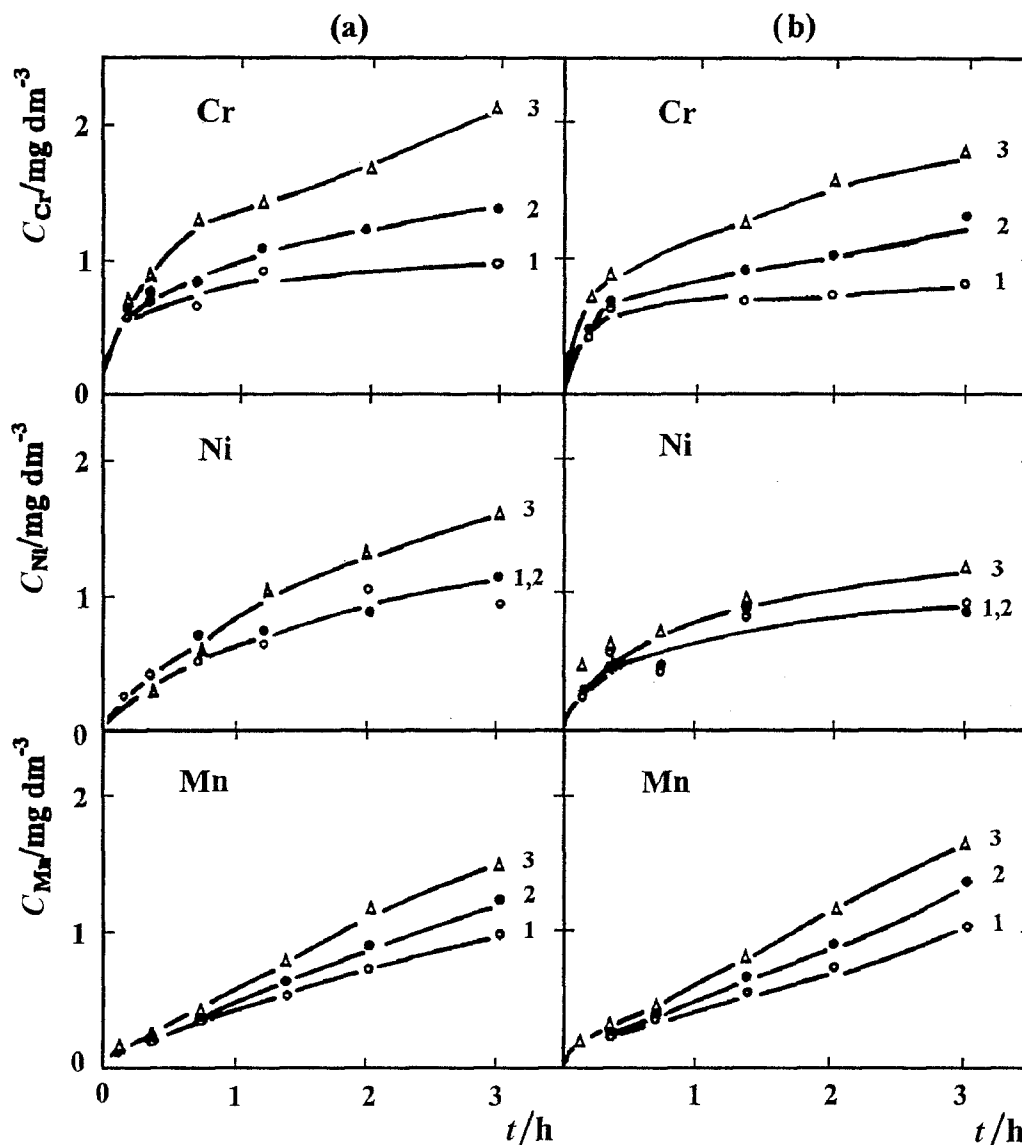


Fig. 9. Time dependence of the dissolution of Cr, Ni and Mn measured by ICP optical emission spectrometer upon spontaneous passivation of duplex stainless steel types (a) 0% Ru and (b) 0.28% Ru in solution consisting of (1)  $0.1 \text{ mol dm}^{-3} \text{ HClO}_4$ ; (2)  $0.1 \text{ mol dm}^{-3} \text{ HClO}_4 + 2 \times 10^{-5} \text{ mol dm}^{-3} \text{ H}_2\text{SO}_4$ ; (3)  $0.1 \text{ mol dm}^{-3} \text{ HClO}_4 + 1 \times 10^{-3} \text{ mol dm}^{-3} \text{ H}_2\text{SO}_4$ .

spontaneous formation of passive layer.) (iii) The dissolution rates of Fe, Cr, Ni and Mn slightly depend on the  $\text{H}_2\text{SO}_4$  concentration of the solution.

In the light of this data, it is possible that passive layers of excellent corrosion resistance are formed on both duplex stainless at the above mentioned experimental conditions. This assumption is strongly supported by the apparently small rate of the dissolution processes, giving an indication that redistribution of the main alloying elements of the surface layers are presumably modest in the course of the spontaneous transformation of duplex steel surfaces.

The  $\Gamma$  against  $E$  curves obtained on the powdered samples of the duplex steels which passivated spontaneously, starting from the open-circuit potential, are shown in Fig. 10. There is no considerable potential dependence of  $\text{HSO}_4^-/\text{SO}_4^{2-}$  accumulations on the steel surfaces in the potential range of 0 to 1200 mV, as depicted by curves 2-2' and 3-3' in Fig. 10. This correlates well to the fact that both of the steels studied exhibit passive features in a wide potential region in  $0.1 \text{ mol dm}^{-3} \text{ HClO}_4$  in the absence and presence of

$\text{H}_2\text{SO}_4$  up to concentration of  $1 \times 10^{-3} \text{ mol dm}^{-3}$  (see Fig. 11). Potential dependence of  $\text{Cl}^-$  sorption shown in curves 1-1' in Fig. 10 does not differ significantly from that of bisulfate/sulfate ions. In this case, following the cathodic polarization curve a potential shift towards more positive values (curve 1') results in a slight increase in the surface excess of  $\text{Cl}^-$  ions. All these results give a further evidence that the extent of the accumulation of aggressive anions decisively depends on the structure and probable composition of the passive layer formed on the surface.

Comparative studies were carried out with surface analytical techniques such as AES and XPS [7] in order to characterize the spontaneous passive films formed on these duplex steels. The passive films formed with and without Ru in HCl and  $\text{H}_2\text{SO}_4$ , clearly show that Cr is moderately enriched in the passive layer. The Cr observed in the spontaneous passive films are mostly in the form of  $\text{Cr}_2\text{O}_3$  and  $\text{Cr}(\text{OH})_3$ , which is normally found in passive layers on stainless steels [8, 9]. While at the outermost range of passive film, the relative amount of  $\text{Cr}(\text{OH})_3$  is prominent,

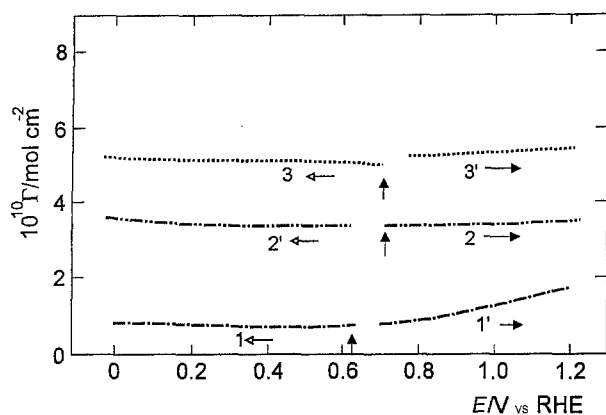


Fig. 10. Potential dependence of  $\text{HSO}_4/\text{SO}_4^{2-}$  and  $\text{Cl}^-$  accumulation in  $0.1 \text{ mol dm}^{-3} \text{ HClO}_4$  under various experimental conditions: (1–1<sup>1</sup>) at  $\text{Cl}^-$  concentration of  $1 \times 10^{-4} \text{ mol dm}^{-3}$  on duplex steel containing 0.28% Ru. (2–2<sup>1</sup>) at  $\text{H}_2\text{SO}_4$  concentration of  $2 \times 10^{-5} \text{ mol dm}^{-3}$  on duplex steel containing 0.28% Ru. (3–3<sup>1</sup>) at  $\text{H}_2\text{SO}_4$  concentration of  $1 \times 10^{-4} \text{ mol dm}^{-3}$  on duplex steel containing 0% Ru. The open-circuit potentials are indicated by arrows.

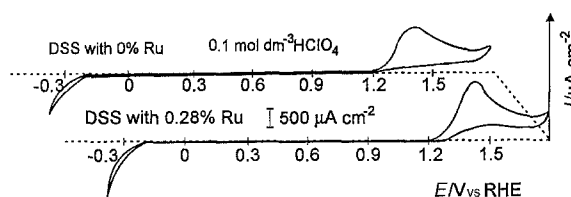


Fig. 11. Cyclic voltammograms of duplex stainless steels in  $0.1 \text{ mol dm}^{-3} \text{ HClO}_4$ . Scan rate:  $20 \text{ mV s}^{-1}$ .

in the deeper region the  $\text{Cr}_2\text{O}_3$  is the predominant contributor to the Cr peak. Analysis by XPS on both steels indicates the existence of various types of iron oxides ( $\text{Fe}_3\text{O}_4$ ,  $\text{Fe}_2\text{O}_3$  and  $\text{FeO}(\text{OH})$ ). It seems that  $\text{Fe}_3\text{O}_4$  and  $\text{Cr}_2\text{O}_3$  contents are higher in the Ru containing samples. A very slight enrichment of the Ni (in metallic Ni form) can also be observed in the sample's surface region. An interesting fact is that only in the case of duplex steel with 0.28% Ru spontaneously passivated in HCl, a significant enrichment of Mo was detected. No Ru enrichment of the passive layers was detected after exposure in either acid solution.

All these results, in accordance with the data presented in [8], suggest that during selective dissolution of Fe the majority of the surface defect sites are initially occupied by Ni, Mo and Cr. It is probable that the surface concentration of Ru also reached a critical value which is found to be below the detection limit of the AES. Both the extent and the strong character of bisulfate/sulfate accumulation are most likely related to the redistribution of these alloying components.

#### 4. Conclusions

The following can be concluded from this investigation:

(i) Small ruthenium additions can significantly increase the corrosion resistance of the duplex stain-

less steels. This is particularly the case if the duplex alloy contains at least 0.22% Ru and is exposed in HCl solutions and at elevated temperature.

(ii) The open-circuit corrosion potential was displaced towards more noble values by the small ruthenium additions in the duplex stainless steel in both the sulphuric and hydrochloric acid solutions used in the investigation.

(iii) The alloys containing ruthenium passivated spontaneously in  $1 \text{ M H}_2\text{SO}_4$  at room temperature, while they all corroded actively in the  $1 \text{ M HCl}$  solution at the same temperature.

(iv) Decreases in the corrosion current densities and critical current densities in the two reducing acid media indicate that ruthenium inhibits the anodic dissolution of the cathodically modified alloys.

(v) Accumulation of  $\text{Cl}^-$  ions on both duplex stainless steel is small (less than  $\Gamma = 1 \times 10^{-10} \text{ mol cm}^{-2}$ ) and their irreversible embedding into the surface oxide layer can be ruled out. The surface excess of bisulfate/sulfate ions is considerably higher (up to  $4.5 \times 10^{-10} \text{ mol cm}^{-2}$ ) as well as their interaction with passive oxide layers seems to be substantially stronger than those of  $\text{Cl}^-$  ions.

(vi) The ruthenium content does not exert significant effects on the sorption behaviours of  $\text{Cl}^-$  and  $\text{HSO}_4/\text{SO}_4^{2-}$  ions on the surfaces of the duplex stainless steels in either type of acid solutions.

#### Acknowledgements

This work was supported by the Hungarian Science Foundation (OTKA grant F4002) and the Ministry of Education (MKM grant 275/92). The authors are grateful to Prof. T. Lengyel (University of Veszprém, Hungary) for discussion and suggestions. One of the authors (W.O.B.) is indebted to Prof. S. Hofmann (Max-Planck-Institut für Metallforschung, Stuttgart) for allowing him to conduct some of the experiments in his laboratories. He also acknowledges the financial support of the Alexander von Humboldt Foundation. Mintek (The Council for Mineral Technology, South Africa) is acknowledged for supplying the alloys used in this investigation.

#### References

- [1] J. H. Potgieter, A. M. Heyns and W. Skinner, *J. Appl. Electrochem.* **20** (1990) 711.
- [2] J. H. Potgieter, *ibid.* **21** (1991) 471.
- [3] *Idem*, *S. Afr. J. Chem.* **46** (1993) 58.
- [4] Annual book of ASTM Standards, vol. 03.02 (1988).
- [5] K. Varga, E. Maleczki, E. Hazi and G. Horanyi, *Electrochim Acta* **35** (1990) 817.
- [6] A. Higginson, R. C. Newman and R. P. M. Proctor, *Corros. Sci.* **29** (1989) 1293.
- [7] W. O. Barnard, K. Varga, P. Baradlai, L. Tomcsanyi and J. H. Potgieter, *Appl. Surf. Sci.* submitted.
- [8] S. C. Tjong, *Appl. Surf. Sci.* **45** (1990) 301.
- [9] N. Sato and G. Okamoto, in 'Comprehensive Treatise of Electrochemistry', vol. 4 (edited by J. O'M. Bockris and B. E. Conway), Plenum Press, New York, (1981).